Published in final edited form as:
Biomaterials. 2011 September ; 32(26): 5957–5969. doi:10.1016/j.biomaterials.2011.03.036.

The hemocompatibility of a nitric oxide generating polymer that catalyzes *S*-nitrosothiol decomposition in an extracorporeal circulation model

Terry C. Major[a,*], **David O. Brant**[a], **Charles P. Burney**[a], **Kagya A. Amoako**[a], **Gail M. Annich**[d], **Mark E. Meyerhoff**[b], **Hitesh Handa**[a,c], and **Robert H. Bartlett**[a]

[a]Department of Surgery, University of Michigan Medical Center, Ann Arbor, MI, USA

[b]Department of Chemistry, University of Michigan, Ann Arbor, MI, USA

[c]Accord Biomaterials, Inc., Ann Arbor, MI, USA

[d]Department of Pediatrics and Communicable Diseases, University of Michigan Medical Center, Ann Arbor, MI, USA

Abstract

Nitric oxide (NO) generating (NOGen) materials have been shown previously to create localized increases in NO concentration by the catalytic decomposition of blood *S*-nitrosothiols (RSNO) via copper (Cu)-containing polymer coatings and may improve extracorporeal circulation (ECC) hemocompatibility. In this work, a NOGen polymeric coating composed of a Cu^o-nanoparticle (80 nm)-containing hydrophilic polyurethane (SP-60D-60) combined with the intravenous infusion of an RSNO, *S*-nitroso-*N*-acetylpenicillamine (SNAP), is evaluated in a 4 h rabbit thrombogenicity model and the anti-thrombotic mechanism is investigated. Polymer films containing 10 wt.% Cu^o-nanoparticles coated on the inner walls of ECC circuits are employed concomitantly with systemic SNAP administration (0.1182 μmol/kg/min) to yield significantly reduced ECC thrombus formation compared to polymer control + systemic SNAP or 10 wt.% Cu NOGen + systemic saline after 4 h blood exposure (0.4 ± 0.2 NOGen/SNAP vs 4.9 ± 0.5 control/SNAP or 3.2 ± 0.2 pixels/cm^2 NOGen/saline). Platelet count (3.9 ± 0.7 NOGen/SNAP vs 1.8 ± 0.1 control/SNAP or 3.0 ± 0.2 × 10^8/ml NOGen/saline) and plasma fibrinogen levels were preserved after 4 h blood exposure with the NOGen/SNAP combination vs either the control/SNAP or the NOGen/saline groups. Platelet function as measured by aggregometry (51 ± 9 NOGen/SNAP vs 49 ± 3% NOGen/saline) significantly decreased in both the NOGen/SNAP and NOGen/saline groups while platelet P-selectin mean fluorescence intensity (MFI) as measured by flow cytometry was not decreased after 4 h on ECC to ex vivo collagen stimulation (26 ± 2 NOGen/SNAP vs 29 ± 1 MFI baseline). Western blotting showed that fibrinogen activation as assessed by Aγ dimer expression was reduced after 4 h on ECC with NOGen/SNAP (68 ± 7 vs 83 ± 3% control/SNAP). These results suggest that the NOGen polymer coating combined with SNAP infusion preserves platelets in blood exposure to ECCs by attenuating activated fibrinogen and preventing platelet aggregation. These NO-mediated platelet changes were shown to improve thromboresistance of the NOGen polymer-coated ECCs when adequate levels of RSNOs are present.

[*]Corresponding author. Department of General Surgery, University of Michigan Health System, 1150 W Medical Center Drive, Ann Arbor, MI 48109, USA. Tel.: +1 (734) 615 5357. tcmajor@umich.edu. .

Keywords

Nitric oxide; Copper nanoparticles; Monocyte CD11b; Platelet P-selectin; Hemocompatible polymer coating; *S*-Nitroso acetylpenicillamine (SNAP)

1. Introduction

The biocompatibility of polymeric tubing used in extracorporeal circulation is highly dependent on the suppression of both the contact coagulation pathway (i.e., fibrin formation) and the activation of circulating blood platelets. Recently, it has been recognized that preventing fibrin formation as well as platelet and monocyte activation while patients are on chronic extracorporeal life support (ECLS), is desirable for increasing the success rate of clinical outcomes. Nitric oxide, an endogenous platelet inhibitor and vasodilator, has already been incorporated into polymeric tubings to mimic its endogenous effects on platelet activation. Indeed, a number of NO releasing (NORel) polymer coatings have been studied over the last decade using polymer-embedded NO donor molecules, such as diazeniumdiolated dibutylhexanediamine (DBHD/N_2O_2) [1–5]. The possible role of NO released locally from polymeric coatings has been found to mediate the level of platelet membrane glycoprotein, P-selectin, and the influence the monocyte integrin, CD11b, in thrombogenicity [1]. However, due to the limited reservoir of the NO donors in the polymer coatings, the NO release approach is only suitable for biomedical devices that require short-term blood ECC contact times, such as hemodialysis and coronary artery bypass surgery, but not for long-term (i.e., weeks or months) of operation. To maintain NO production for extended periods of time it may be possible to take advantage of endogenous species such as nitrosothiols (RSNO) that are constantly produced endogenously (from NO generated by nitric oxide synthase) to produce NO *in situ* at a polymer/blood interface.

Nitric oxide generating (NOGen) polymers contain an immobilized catalyst such as copper (Cu) nanoparticles or a Cu(II) ion/ligand complex that can liberate NO from circulating *S*-nitrosothiols (RSNO) at the blood/polymer interface [6–9]. RSNOs, which serve as intermediates in the metabolism and transport of biologically active NO, can exist in two forms, the diffusion-limited high molecular weight (HMW) RSNOs such as *S*-nitroso-albumin and the more mobile low molecular weight (LMW) RSNOs such as *S*-nitrosocysteine and *S*-nitrosoglutathione [10]. Scharfstein et al. reported that the transfer of NO or transnitrosylation between the HMW and the LMW RSNOs occurs rapidly and completely under physiological conditions [10]. The effectiveness of the NOgen polymers to release NO is dependent upon the level of reduced catalyst (Cu(I)) and the availability of LMW RSNOs to the catalytic Cu(I) species after its reduction from Cu(II). The redox cycling of Cu(II) and Cu(I) and then back to Cu(II) if other reducing agents like thiols and ascorbate are present Eq. (1) can provide a continuous NO generation from LMW RSNOs as long as the total circulating RSNO level is maintained at adequate levels through exogenous RSNO delivery and transnitrosylation processes [11–15].

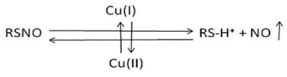

(1)

However, the effects of the NO produced from circulating RSNOs, after contact with the NOGen polymer coatings, on preserving platelet count and function remains unclear.

To test the hypothesis that sustainable NO generation (NOGen) due to the catalytic decomposition of RSNOs mediates circulating platelet and monocyte quiescence, the present study was designed to evaluate if platelet P-selectin and monocyte CD11b expressions are preserved by the NO released from the copper nanoparticle doped polymer-coated ECC circuits and exogenous SNAP. The copper nanoparticles within the polymer coatings can slowly corrode to produce sparingly soluble oxides and other copper salts that provide low levels of catalytically active Cu(I)/Cu(II) ions at polymer/solution interfaces. The copper ions can then interact with RSNOs in the flowing blood to locally produce elevated levels of NO. Therefore, we investigated, in a rabbit model, if the preservation of platelets was mediated by direct platelet attenuation as measured by platelet membrane P-selectin expression and/or a conformational change in plasma fibrinogen as measured by the Aγ dimer formation after 4 h of blood exposure to NOGen ECC circuits formulated with copper nanoparticles.

2. Materials and methods

2.1. Materials

Tygon® poly(vinyl chloride) (PVC) tubing was purchased from Fisher Healthcare (Houston, TX). The tecophilic polyurethane, SP-60D-60, was a product of Lubrizol Advanced Materials, Inc. (Cleveland, OH). Tetrahydrofuran (THF) was obtained from Sigma–Aldrich Chemical Co. (St.Louis, MO). Copper nanoparticles (80 nm) were obtained from Sigma–Aldrich (St. Louis, MO). The mouse antibodies for human CD61 (GPIIIa) FITC and human P-selectin glycoprotein (CD62P) PE were from AbD Serotec (Raleigh, NC) as well as Mouse isotype controls for IgG_1 FITC and IgG_1 PE. For monocyte surface receptor determination of the integrin, CD11b, and the surface antigen CD14, the rat antibody for mouse CD11b Alexa Flour 488 and mouse antibody for human CD 14 PE, respectively, from AbD Serotec were used. The antibody clones for P-selectin, CD11b and CD14 have been previously shown to have cross-reactivity to the rabbit [16–19]. The rat isotype control for IgG_{2b} Alexa Fluor 488 and the mouse isotype control for IgG_{2a} PE were purchased from AbD Serotec. Human plasma fibrinogen containing ≥90% clottable proteins was obtained from Calbiochem (La Jolla, CA) and fluorescein-labeled goat IgG (polyclonal) against denatured human fibrinogen was purchased from MP Biomedicals, LLC (Solon, OH). The 96-well microtiter plates (black, polypropylene) used for fluorescence measurements were obtained from Nalge Nunc International (Rochester, NY). All other reagents were of the highest purity available.

2.2. Preparation of NOGen polymeric coatings and ECC construction

A polymer coating solution containing 1, 5 and 10 wt.% copper nanoparticles in SP-60D-60 polyurethane was prepared using a method previously reported [7]. Briefly, double layers of polymeric coatings which included an active layer and a top layer were individually coated on the inner wall of the Tygon® tubing that formed the ECC. The active layer was prepared by dissolving 700 mg SP-60D-60 in 12 ml THF along with 1–10 wt.% copper nanoparticles (Soln A). Copper nanoparticles were sonicated in THF before mixing with the SP-60D-60/THF solution to obtain a more uniform dispersion. The top layer was formulated using 700 mg SP-60D-60 in 12 ml THF (Soln B).

The ECC configuration used in this study was previously described [1]. The ECC consisted of a 16-gauge and 14-gauge IV polyurethane angiocatheters (Kendall Monoject Tyco Healthcare Mansfield, MA), two 16 cm lengths of ¼ inch inner diameter (ID) Tygon® tubing and a 8 cm length of 3/8 inch ID Tygon® tubing which created a thrombogenicity chamber where thrombus could form more easily due to more turbulent blood flow. The ECC was pieced together, starting at the left carotid artery side, with the 16-gauge

angiocatheter, one 15 cm length ¼ inch ID tubing, the 8 cm length thrombogenicity chamber, the second 15 cm length ¼ inch ID tubing and finally the 14-gauge angiocatheter. The angiocatheters were interfaced with tubing using 2 luer-lock PVC connectors. The 3/8 inch ID tubing and the ¼ inch tubing were welded together using THF.

The assembled ECC was coated first with two active coats of Soln A, followed by one top coat of Soln B. The circuitry was filled with each solution then removed. Each coat was allowed to dry for at least 1 h. The finished ECCs were allowed to cure under nitrogen conditions for 20 min, and then dried under vacuum for 2 d. (Fig. 1B).

2.3. NO release measurements

NO released from the NOGen polymer-coated circuits was measured via a Sievers chemiluminescence NO Analyzer® (NOA), model 280 (Boulder, CO). as described previously [7]. Briefly, *S*-nitrosoglutathione (GSNO), used as the substrate for the copper-containing polymer, was prepared by the reaction of equimolar glutathione (GSH) and $NaNO_2$ in 0.06 M H_2SO_4. The prepared GSNO (1 μM), 30 μM GSH and 5 μM EDTA, which was used to chelate any contaminant metal ions, were added to an amber reaction vessel containing phosphate-buffered saline (PBS) at 37 °C. After a 5 min measurement of baseline NO level, a centimeter square sample of the copper-containing circuitry was then placed in the reaction vessel containing the substrate solution at 37 °C. NO was continuously swept from the headspace of the sample vessel and purged from the bathing solution with a nitrogen sweep gas and bubbler into the chemiluminescence detection chamber. The flow rate was set to 200 ml/min with a chamber pressure of 5.4 Torr and an oxygen pressure of 6.0 psi. Using this method, a uniform segment of NOGen polymer was tested for NO release prior to and 4 h after blood exposure.

2.4. In vitro fibrinogen adsorption assay

The *in vitro* fibrinogen adsorption immunofluorescence assay was performed in a 96-well format. The NOGen and control polymer solutions used in preparing the ECC was also used to coat microwells of the 96-well microtiter plates. In addition, similar polymer drying conditions were used for the ECC and 96-well preparations. Briefly, human fibrinogen was diluted to 3 mg/ml with Dulbecco's phosphate-buffered saline (dPBS) without $CaCl_2$ and $MgCl_2$ (Gibco Invitrogen Grand Island, NY), equivalent to the human plasma concentration, and then used for the adsorption experiments [20]. One hundred μl of this solution were added to each well for 1.5 h at 37 °C, followed by eight washing steps using 100 μl of wash buffer, which consisted of a 10-fold dilution of AbD Serotec Block ACE buffer (Raleigh, NC) and 0.05% Tween 20 (Calbiochem La Jolla, CA). To block nonspecific antibody binding, wells were incubated with 100 μl blocking buffer (4-fold dilution of Serotec Block ACE buffer) for 30 min at 37 °C. After rinsing 3 times with wash buffer (100 μl per well) a background fluorescence measurement of the plates was performed at 485 nm (excitation) and 528 nm (emission) on a Synergy 2 fluorescence microplate reader (Biotek Winooski, VT). To detect the adsorbed fibrinogen, goat anti-human fibrinogen antibody was diluted (1:10) in a 10-fold dilution of the Serotec Block ACE buffer and 100 μl of this final solution was added to each well. The antibody was allowed to bind to the surface-adsorbed fibrinogen for 1.5 h at 37 °C. Human fibrinogen adsorption to non-coated polypropylene was used as an internal control to normalize the fluorescence signals within different plates. A standard curve for fibrinogen was obtained on each plate from 0 to 3000 μg/ml. All measurements were done in triplicate and performed with the Synergy 2 fluorescence reader.

2.5. The rabbit thrombogenicity model

The animal handling and surgical procedures were approved by the University Committee on the Use and Care of Animals in accordance with university and federal regulations. A

total of 32 Zealand white rabbits (Myrtle's Rabbitry, Thompson's Station, TN) were used in this study. All rabbits (2.5–3.5 kg) were initially anesthetized with intramuscular injections of 5 mg/kg xylazine injectable (AnaSed® Lloyd Laboratories Shenandoah, Iowa) and 30 mg/kg ketamine hydrochloride (Hospira, Inc. Lake Forest, IL). Maintenance anesthesia was administered via a diluted intravenous (IV) infusion of ketamine (2 mg/ml) at a rate of 2.62 mg/kg/h. In order to maintain blood pressure stability, IV fluids of Lactated Ringer's were given at a rate of 33 ml/kg/h. The paralytic, pancuronium bromide (0.33 mg/kg, IV), was administered to have animal totally dependent upon mechanical ventilation which was done via a tracheotomy and using a Sechrist Infant Ventilator Model IV-100 (Anaheim, CA). For monitoring blood pressure and collecting blood samples, the rabbits' right carotid artery was cannulated using a 16-gauge IV angiocatheter (Jelco®, Johnson & Johnson, Cincinnati, OH). Blood pressure and derived heart rate were monitored with a Series 7000 Monitor (Marquette Electronics Milwaukee, WI). Body temperature was monitored with a rectal probe and maintained at 37 °C using a water-jacketed heating blanket. Prior to placement of the arteriovenous (AV) custom-built extra-corporeal circuit (ECC), the rabbit left carotid artery and right external jugular vein were isolated and baseline hemodynamics as well as arterial blood pH, pCO_2, pO_2, total hemoglobin and methemoglobin were measured using an ABL 725 blood-gas analyzer and an OSM3 Hemoximeter (Radiometer Copenhagen Copenhagen, DK). In addition, baseline blood samples were collected for platelet and total white blood cell (WBC) counts which were measured on a Coulter Counter Z1 (Coulter Electronics Hialeah, FL). Plasma fibrinogen levels were determined using a Dade Behring BCS Coagulation Analyzer (Siemans Deerfield, IL), activated clotting times (ACT) were monitored using a Hemochron Blood Coagulation System Model 801 (International Technidyne Corp. Edison, NJ), platelet function was assessed using a Chrono-Log optical aggregometer model 490 (Havertown, PA) and platelet P-selectin and monocyte CD11b expression were determined utilizing fluorescent-activated cell sorting (FACS) with a Becton Dickinson FACSCalibur flow cytometer (San Jose, CA).

After baseline blood measurements, the AV custom-built ECC was placed into position by cannulating the left carotid artery for ECC inflow and the right external jugular vein for ECC outflow. The flow through the ECC was started by unclamping the arterial and venous sides of ECC and blood flow in circuit was monitored with an ultrasonic flow probe and flow meter (Transonic HT207 Ithaca, NY). Animals were not systemically anticoagulated during the experiments. For 1, 5 and 10 wt.% of the copper nanoparticle-coated ECC studies, 0.1182 μmol/kg/min infusion of the RSNO, SNAP, was started after the ECC blood flow was initiated. A separate group of animals, consisting of 10 wt.% copper-coated ECC plus a 0.0591 μmol/kg/min infusion (i.e., ½ RSNO dose) of SNAP, was evaluated.

After 4 h on ECC plus either saline or SNAP infusion, the circuits were clamped, removed from animal, rinsed with 60 ml of saline and drained. Any residual thrombus in the larger tubing of ECC (i.e., thrombogenicity chamber) was photographed and the degree of thrombus image was quantitated using Image J imaging software from National Institutes of Health (Bethesda, MD). Prior to euthanasia, all animals received a dose of 400 U/kg sodium heparin to prevent necrotic thrombosis. The animals were euthanized using a dose of Fatal Plus (130 mg/kg sodium pentobarbital) (Vortech Pharmaceuticals Dearborn, MI). All animals underwent gross necropsy after being euthanized, including examination of the lungs, heart, liver and spleen for any signs of thromboembolic events.

2.6. Blood sampling

Rabbit whole blood samples were collected in non-anticoagulated 1 cc syringes for ACT, 10% anticoagulant containing sodium citrate, sodium phosphate and dextrose (ACD) (Hospira,Inc. Lake Forest, IL) in 3 cc syringes for cell counts, aggregometry and FACS analysis, and 1 cc syringes containing 40 U/ml of sodium heparin (APP Pharmaceuticals,

LLC Schaumburg, IL) for blood-gas analysis. Following the initiation of ECC blood flow, blood samples were collected every hour for 4 h for *in vitro* measurements. Samples were used within 2 h of collection to avoid any activation of platelets, monocytes or plasma fibrinogen.

2.7. Platelet aggregometry

Rabbit platelet aggregation was assayed based on the Born's turbidimetric method using a Chrono-Log optical aggregometer as previously described [1]. Briefly, citrated blood (1:10 blood to ACD) was collected (6 ml) and platelet-rich plasma (PRP) was obtained by centrifugation at 110× *g* for 15 min. Platelet-poor plasma (PPP) was obtained by another centrifugation of the PRP-removed blood sample at 2730× *g* for 15 min and was used as the blank for aggregation. PRP was incubated for 10 min at 37 °C and then 40 μg/ml collagen (Chrono-PAR #385 Havertown, PA) was added. The percentage of aggregation was determined 3 min after the addition of collagen using Chrono-Log Aggrolink software.

2.8. Flow cytometry

To determine platelet P-selectin (CD62P) and IIb/IIIa (fibrinogen receptor) expression, 100 μl of diluted blood aliquots (1:100 dilution of blood to Hank's Balanced Salt Solution (HBSS) without $CaCl_2$ and $MgCl_2$) were directly prepared for cell surface staining of P-selectin and IIb/IIIa. In four 12 × 75 polypropylene tubes containing 100 μl of diluted blood, 40 μg/ml collagen (4 μl 1000 μg/ml) was added to two tubes and 4 μl saline was added to the other two tubes. At this point, saturating concentrations (10 μl) of monoclonal anti-human IIIa FITC and monoclonal anti-human CD62P PE antibodies were added to one of the collagen and one of the saline treated tubes and incubated for 15 min at room temperature (RT) in the dark. In the other two tubes containing collagen and saline, 10 μl each of anti-mouse IgG_1 FITC and PE were added as nonbinding isotype controls and also incubated for 15 min at RT in the dark. After the antibody incubation step, each tube received 700 μl of freshly prepared 1% formaldehyde buffer (in dPBS) and was stored at 4 °C until ready for flow cytometric analysis. To determine monocyte CD11b and CD14 expression, 100 μl of the undiluted blood aliquots were directly prepared for cell surface staining of CD11b and CD14. At this point, saturating concentrations (10 μl) of rat anti-mouse CD11b Alexa Fluor 488 and monoclonal anti-human CD14 PE antibodies were added to one tube and 10 μl each of anti-rat IgG_{2b} Alexa Fluor 488 and anti-mouse IgG_{2a} PE were added as nonbinding isotype controls. All tubes were incubated for 30 min at 4 °C in the dark. After the antibody incubation, lysing of red blood cells was accomplished by adding 2 μl of FACSLysing Buffer (Becton Dickinson San Jose, CA), gentle vortexing and then incubating for 10 min at room temperature in the dark. After red blood cell lysing, centrifugation at 250× *g* for 5 min at 4 °C pelleted the stained leukocytes. After aspirating supernatant, one wash step was done with wash buffer containing dPBS, 0.1% sodium azide and 0.5% bovine serum albumin, and then the the sample was centrifuged again and the resulting supernatant was aspirated. The cells were then resuspended in 250 μl of freshly prepared 1% formaldehyde buffer and stored at 4 °C until ready for flow cytometric analysis. A FACSCalibur flow cytometer (Becton Dickinson San Jose, CA) was used for the acquisition of flow data and the CellQuest software was employed for data analysis. Cell populations were identified for data collection by their forward scatter (FSC) and side scatter (SSC) light profiles. For each sample, 30,000 total events were collected. Fluorescence intensity of immunostaining was quantitated by a histogram log plot analysis. Mean fluorescent intensity (MFI) was expressed as the geometric mean channel fluorescence minus the appropriate isotype control.

2.9. In vitro plasma copper assay

The *in vitro* plasma copper assay (DICU-250, Gentaur, Accurate Chemical & Scientific Corporation York, NY) was performed in a 96-well format to determine the amount of copper leaching into the blood of the rabbits from the ECC over the 4 h experimental period. Briefly, both baseline and 4 h plasma samples were treated with 30% trichloroacetic acid. Samples were centrifuged at 14,000 RPM for 5 min and 100 μl of the supernatant was collected. Each sample was diluted 1:2 with deionized water and 100 μl placed in a 96-well plate. A copper standard (1.5 mg/dl $CuSO_4$) was serial diluted and 100 μl of each concentration, ranging from 0 to 300 μg/dl, was placed in separate wells. A working reagent mix containing 0.9% ascorbic acid, 0.1% 4,4′-dicarboxy-2,2′-biquinoline, 2% NaOH and 8% Hepes-free acid was then added to each well of the 96-well plate and mixed. After a 5 min incubation, absorbance measurement of the plate was performed at 359 nm on a Synergy 2 microplate reader (Biotek Winooski, VT). All measurements were done in duplicate. Using a linear regression curve from a copper standard (0–300 μg/dl), sample copper concentrations were calculated. In addition, to determine the long-term copper leaching levels from the NOGen polymer-coated ECC, an *in vitro* study which involed serially sampling saline bathing solution that was equilibrated withiin the ECC for up to7 d was carried out.

2.10. Plasma fibrinogen Aγ dimer expression via Western immunoblot

Plasma from the citrated whole rabbit blood collected over the 4 h experimental period for each NOGen or control polymer coating plus infusion of either SNAP or saline was used for a Western blot analysis of plasma fibrinogen Aγ dimer expression. After the −70 °C-stored samples were rapidly thawed in a 37 °C water bath, an aliquot of 0.2 μl of plasma mixed with Laemmli sample buffer containing 2% β-mercaptoethanol and incubated for 5 min at 95 °C were run on a 7.5% sodium dodecyl sulfate-polyacrylamide gel using a Bio-Rad miniblot electrophoresis system (Criterion Hercules, CA). Protein was transferred onto poly(vinyl-difluoride) membranes for 2 h at 1 amp. Membranes were blocked with Tris-buffered saline containing 0.05% Tween 20 and 3% nonfat dry milk (Bio-Rad) for 1 h at room temperature followed by an overnight incubation at 4 °C with FITC conjugated goat anti-human fibrinogen antibody with gentle rocking. The membranes were washed twice for 10 min each and then imaged in a fluorescence imager (Bio-Rad VersaDoc MP4000 Hercules, CA). The Aγ and γ fibrinogen subunit densities were quantified using Quantity One software (Bio-Rad). The Aγ dimer density was calculated as a ratio of the Aγ dimer band over the sum of dimers plus monomers.

2.11. Statistical analysis

Data are expressed as mean ± SEM (standard error of the mean). Comparison between the various wt.% of NOGen and control polymer groups were analyzed by the one-way ANOVA with a multiple comparison of means using Student's *t*-test. All statistical analyses were performed using the statistical program SAS JMP (SAS Institute Cary, NC). The immunoblot analysis of the Aγ dimer expression was statistically compared by the Student's *t*-test. Values of $P < 0.05$ were considered statistically significant for all tests.

3. Results

3.1. Cu^{o}-nanoparticle/SP-60D-60 polyurethane (NOGen) polymer characteristics

It is well known that copper ions can catalyze the reduction of *S*-nitrosothiols to NO. Hence, initially a NOGen polymer that contained a lipophilic Cu(II) complex (analogue to cyclen) shown in Fig.1A (Cu(II)-dibenzo[e,k]-2,3,8,9-tetraphenyl-1,4,7,10-tetra-azacyclododeca-1,3,7,9-tetraene (Cu(II)-DTTCT)) incorporated at 5 wt.% into plasticized

PVC was evaluated as the inner wall coating in the rabbit extracorporeal circulation (ECC) model. After 4 h of blood exposure the Cu(II) ligand complex showed marked reduction in NO release (0.5–1 vs >20 × 10^{-10} mol cm^{-2} min^{-1} baseline) and platelet count (data not shown). This was traced to significant heterogeneity of the lipophilic complex on the surface, and subsequent sloughing off and/or passivation of the copper(II) complex active material. An improved NOGen polymer was constructed that incorporated copper nanoparticles in a hydrophilic polyurethane (Fig. 1B) that would allow Cu(II) ions to be generated locally via very slow corrosion of the nanparticles to form trace levels of catalytic copper ions to generate NO from the circulating RSNOs. Therefore, these copper particle-containing NOGen polymer coatings were used for the rest of the ECC studies reported herein. The mechanism of NO generation is dependent upon the polymer being hydrophilic, and thereby allowing both the blood-borne low molecular weight *S*-nitrosothiols, such as *S*-nitrosocysteine and *S*-nitrosoglutathione, to come in contact with the reduced ionized Cu (I) species and generate NO from the RSNOs (Fig. 2A) (in the hydrophilic PU layer) before these ions are completely scavenged by proteins in the plasma phase of the blood. The NO generated from the circulating *S*-nitrosothiols by the copper-containing polymer make it a reasonable material because of the potential unlimited supply of generated NO at levels that exceeds the physiological NO release from endothelial cells (0.5–4 × 10^{-10} mol cm^{-2} min^{-1}) [21]. As shown in Fig. 2B, NO generation from ECC circuits with the NOGen polymer, as measured via a chemiluminescence NO analyzer, was obtained by adding 1 μM GSNO to the piece of NOGen polymer-coated tubing. The 1, 5 and 10 wt.% copper particle polymers provided NO fluxes that peaked at 5 ± 1, 10 ± 2 and 12.4 ± 2 × 10^{-10} mol cm^{-2} min^{-1}, respectively. The ability of the coating to release steady-state levels of NO in physiological buffer was achieved for the 4 h period by the continuous IV infusion of an RSNO, SNAP, during the ECC procedure. Most importantly, it was confirmed that the NO released from the NOGen ECC was not significantly reduced after 4 h of blood exposure, as shown in Fig. 2B. Indeed, a piece of tubing removed from the circuit post-experiment and measured for NO generation in the presence of GSNO, yielded nearly the same or slightly less NO compared to the pre-blood exposure levels. This suggests that the blood environment (i.e., proteins, cells, etc.) did not alter the kinetics of the NO release from the Cu^{o}-nanoparticle-containing NOGen coating.

To determine if plasma protein adsorption and in particular, human fibrinogen, occurs with this polymer, an *in vitro* immunofluorescence assay was performed. The NOGen polymer coatings (1, 5 and 10 wt.% Cu(II) particle NOGen polymer) exhibited significant human fibrinogen adsorption compared to the non-nanoparticle control polymer (Fig. 3). The adsorption of the human fibrinogen to the 5 and 10 wt.% Cu(II) particle polymers were similar.

Since Cu(I/II) ions are released from the Cu nanoparticles in an aqueous environment, Cu corrosion occurs at the polymer coating surface which leads to leaching of Cu(II) and Cu(I) ions into the systemic circulation. The question at this point is what amount of Cu(II) ions are actually present in the systemic circulation after the 4 h blood exposure and to determine this level of copper ions in the plasma via a colorimetric plasma copper assay. After 4 h of blood flow, the 1, 5 and 10 wt.% Cu particle polymer ECCs demonstrated a 1, 1.2 and 1.3 fold increase, respectively, in total plasma copper concentrations compared to the baseline (i.e., no ECC present) plasma copper levels with either SNAP or saline systemic infusion (Fig. 4A). The non-Cu^{o}-nanoparticle control ECC plus SNAP actually showed a reduction in plasma concentration of Cu(II) compared to the baseline levels (122 ± 13 vs 178 ± 5 μg/dl, respectively). In addition, if the rate of Cu(I/II) leaching into the plasma from the Cu^{o}-nanoparticle doped polymer coating is 1.3 fold increase after 4 h what would be the leaching be after 24 h or even 7 days? As shown in Fig. 4B the copper concentration was measured in saline which resided in 10 wt.% Cu particle polymer-coated and non-Cu particle control

ECCs for up to 7 d at room temperature. As expected, the non-Cu^0-nanoparticle control ECCs had no Cu(II) present over the 7 d. The 10 wt.% Cu particle ECC did accumulate up to 23.4 ± 8 μg/dl Cu(II) in the saline solution after 7 d. The 4 h accumulation was 5.9 ± 6.2 μg/dl which indicates a very slow rate of copper corrosion to copper ions within the coatings containing the copper nanoparticles.

3.2. Effects of NOGen polymer plus SNAP infusion on rabbit hemodynamics and thrombus formation

Hemodynamic effects of 10 wt.% Cu^0-nanoparticle NOGen- and non-Cu^0-nanoparticle control-coated ECC plus SNAP infusion over 4 h of blood exposure in the rabbit model of thrombogenicity are shown in Table 1. Maximal hemodynamic effects were observed with the 10 wt.% Cu particle polymer due to the maximal NO generation potential of this material. Mean arterial blood pressure (MAP) within 2 h on ECC significantly fell when using the 10 wt.% NOGen/SNAP group but returned to baseline levels after 4 h. This returned in MAP to baseline is due to the continuous IV fluid maintenance at 33 ml/kg/h. Heart rate for the NOGen and control ECC groups were unchanged over the 4 h. The blood flow through the ECC was dependent upon MAP and after 4 h increased due to the added IV fluids. Not unexpected, the activated clotting time (ACT) after 4 h on the NOGen or control polymer ECCs increases, probably due to the increase in intravascular fluids, i.e., hemodilution effect. The total white blood cell (WBC) count remained unchanged over the 4 h for either ECC group of animals. The total WBC count is composed of lymphocytes, monocytes and granulocytes.

To ascertain the differential formation of thrombus in the thrombogenicity chamber (i.e., the 3/8 inch ID Tygon tubing 8 cm in length) of the 1, 5, 10 wt.% NOGen or non-Cu^0-nanoparticle control polymer-coated ECC, 2-dimensional (2D) image analysis was performed after 4 h of blood exposure. The thrombus area was analyzed by using the Image J imaging software and represents the 2D area of thrombus formation (pixels/cm^2) in each tubing chamber. These thrombi area measurements were quantitated and, as shown in Fig. 5, the thrombus area of the 5 and 10 wt.% Cu^0-nanoparticle NOGen polymer ECC/SNAP infusion were significantly smaller when compared to the non-Cu^0-nanoparticle control polymer ECC plus SNAP. Interestingly, the half-dose of SNAP plus the 10 wt.% Cu^0-nanoparticle NOGen polymer ECC also had a significant reduction in the thrombus formation. However, 10 wt.% Cu^0-nanoparticle polymer/saline formed as much thrombus as the non-Cu^0-nanoparticle control plus a full dose of SNAP. Thus, only when the copper nanoparticle doped coating is used in combination with exogenous addition of RSNOs to the blood, can a significant reduction in thrombus formation be observed. This suggests that the levels of endogenous RSNOs are not adequate to produce the surface of levels of NO required to substantially decrease platelet activation and subsequent thrombus formation.

3.3. Effects of NOGen polymer and SNAP infusion on rabbit platelet function and surface receptor expressions

Platelet function during exposure to NOGen and control polymer-coated ECC was assessed by observing platelet count (Fig. 6A) and the level of plasma fibrinogen, to which activated platelets bind (Fig. 6B). Both platelet count and plasma fibrinogen levels were corrected for hemodilution due to the added IV fluids. The 10 wt.% Cu^0-nanoparticle NOGen polymer-coated ECC plus SNAP infusion showed the greatest preservation of platelet count and plasma fibrinogen levels over the course of the 4 h blood exposure while the non-copper particle control polymer ECC plus SNAP showed a time-dependent loss in platelet count and plasma fibrinogen levels. The 10 wt.% Cu^0-nanoparticle NOGen ECC/SNAP was able to maintain platelet counts to 90% or greater even at 3 and 4 h of blood exposure when compared to the non Cu^0-nanoparticle control polymer ECC/SNAP (Fig. 6A). Both the 1

and 5 wt.% Cu^o-nanoparticle NOGen ECCs plus SNAP infusion did not preserve platelets to the same degree as the 10 wt.% Cu particle/SNAP group. In Fig. 6B, plasma fibrinogen levels are shown to be unchanged in both the 10 wt.% Cu^o-nanoparticle NOGen with full or half-dose of SNAP compared to the non-Cu^o-nanoparticle control ECCs plus SNAP. Interestingly, there was no difference between the 1 and 5 wt.% Cu^o-nanoparticle NOGen coatings plus SNAP and the non-Cu^o-nanoparticle control polymers and SNAP in their ability to preserve plasma fibrinogen at any time point.

The percent of platelet functional aggregation, as determined by ex vivo collagen (40 μg/ml) stimulation of PRP, was measured by optical turbidity (Fig. 7). The ability of platelets to aggregate was only maintained with the 10 wt.% Cu^o-nanoparticle NOGen polymer ECC plus half-dose of SNAP whereas platelets from the 10 wt.% Cu^o-nanoparticle ECC plus full dose of SNAP were significantly reduced in their ability to aggregate upon collagen stimulation, especially at the 3 and 4 h time points (Fig. 7).

To ascertain if the observed reduction in platelet aggregation with the 10 wt.% Cu^o-nanoparticle NOGen polymer after 4 h blood exposure was due to direct effects on platelet activation, expression of the platelet membrane adhesion glycoprotein, P-selectin (CD62P), was measured by fluorescence-activated cell sorting (FACS) analysis. When platelets become activated, the surface expression of P-selectin increases [22]. As shown in Fig. 8A, the unstimulated P-selectin expression was unchanged after 4 h for all experimental groups except the 10 wt.% Cu^o-nanoparticle plus saline group which showed an increase in unstimulated P-selectin expression as compared to the unstimulated (i.e., no exogenous collagen) baseline (no ECC present). However, 40 μg/ml collagen significantly stimulated an increase in P-selectin expression at baseline and after 4 h for all NOGen ECC groups. The collagen-stimulated P-selectin expression for the 4 h time point for the 10 wt.% Cu^o-nanoparticle ECC plus saline had an increase in P-selectin of 10 ± 3 mean fluorescence intensity (MFI) while the 1,5,10 wt.% Cu^o-nanoparticle NOGen ECC with a full dose of SNAP and 10 wt.% Cu^o-nanoparticle NOGen ECC plus a half-dose of SNAP were significantly increased 16 ± 1, 18 ± 2, 13 ± 2 and 19 ± 1 MFI, respectively, from the collagen-stimulated baseline (no ECC) levels.

In order to understand if the Cu^o-nanoparticle-containing NOGen polymer can induce changes in the IIb/IIIa (fibrinogen) receptor, a specific antibody to IIIa (CD61) was used to evaluate platelet surface expression of IIb/IIIa via flow cytometry. As shown in Fig. 8B, the platelet IIIa surface expression after 4 h for all NOGen ECC groups was unchanged compared to the no ECC baseline levels. The IIIa expression, however, significantly increased with 40 μg/ml exogenous collagen at baseline and after 4 h for all NOGen ECC groups.

3.4. Effects of NOGen polymer on rabbit surface receptor expressions of monocytic integrin, CD11b, and the constitutive monocyte-specific receptor, CD14

To determine if the NOGen polymer in the ECC can increase the surface integrin, CD11b, expression on circulating monocytes that translates into activated monocytes, FACS analysis of rabbit whole blood at baseline (no ECC) and after 4 h of circuit blood exposure was performed. An increase in CD11b expression on circulating monocytes indicates a response to an early inflammatory event [23]. The CD11b expression on rabbit monocytes was observed to significantly increase 3-fold after 4 h blood exposure to the control polymer ECCs, but all Cu^o-nanoparticle-containing NOGen polymer ECCs exhibited no change in the CD11b expression from the no ECC baseline situation (Fig. 9). The CD11b expression observed with the NOGen polymer 4 h after blood exposure was also significantly reduced from that observed after 4 h on control polymer ECC. If the circulating monocytes are becoming activated, as indicated by the increase in CD11b expression, then the number of

circulating monocytes as marked by the constitutive surface receptor, CD14, should be decreased. After 4 h of blood exposure the non-Cu^o-nanoparticle control ECC plus SNAP did show a significant decrease in CD14 expression indicating a loss of circulating monocytes compared to the no ECC baseline levels. The Cu^o-nanoparticle-containing NOGen ECCs with SNAP or saline showed no change from baseline in the number of circulating monocytes after 4 h of blood exposure.

3.5. Effects of NOGen polymer on Aγ dimer formation in plasma fibrinogen

In order to determine why 10 wt.% Cu^o-nanoparticle ECC plus SNAP infusion would attenuate platelet aggregation but maintain normal expression of platelet P-selectin, activation of plasma fibrinogen was investigated for an increase in the amount of Aγ heterodimer by Western immunoblot assay. In the biosynthesis of fibrinogen, the formation of Aγ heterodimers linked by disulfide bonds is suggested to be an intermediate in the assembly of fibrinogen [24]. Conformational changes in fibrinogen structure via equilibria between thiols and disulfide bonds have been observed and found to inhibit thrombin-catalyzed fibrinogen polymerization [25]. In Fig. 10, when plasma samples from animals exposed to 10 wt.% Cu^o-nanoparticle ECC plus SNAP, non-Cu^o-nanoparticle ECC plus SNAP, and the 10 wt.% Cu^o-nanoparticle plus saline infusion were run on a reduced SDS-PAGE gel, the percent level of the Aγ dimer to total Aγ dimer + γ monomer was significantly reduced in the case of the 10 wt.% Cu^o-nanoparticle NOGen/SNAP group when compared to either the non-Cu^o-nanoparticle ECC/SNAP or 10 wt.% Cu^o-nanoparticle ECC/saline groups.

4. Discussion

In vivo testing of the Cu^o-nanoparticle-containing polymer coating in an extracorporeal circuit with exogenous RSNOs demonstrated that the NOGen polymer can generate NO, preserve platelet count and maintain monocyte inactivation after at least 4 h of blood exposure in a rabbit model of thrombogenicity. However, even though overall platelet number was preserved, functional platelet aggregation was inhibited with the 10 wt.% Cu^o-nanoparticle-coated ECC plus exogenous SNAP addition after the 4 h of blood exposure. Direct platelet activation, in contrast, was not inhibited by the NOGen polymer and SNAP infusion as measured by the platelet surface glycoprotein, P-selectin, expression but the platelets did respond to exogenous collagen in a fashion similar to a no ECC sample. In order for platelets to have a normal response to an agonist stimulation such as collagen but have an inhibited aggregation response would indicate that some plasma factor promoting platelet aggregation might be adversely affected by both the NO generated by the NOGen polymer and the excess RSNOs present in the platelet-rich plasma (PRP). Since plasma fibrinogen is the protein the actively binds to activated platelets and provides the means for platelet aggregation, alterations in plasma fibrinogen, and not the platelets per se, might be a basis for the preservation of platelets and enhanced hemocompatibility of the 10 wt.% Cu^o-nanoparticle NOGen polymer plus SNAP in the extracorporeal circuit.

Previous work, including ours, has established that NO releasing polymers (NORel) can prevent loss of circulating platelets and monocytes [1,5,26–32]. This provides significant evidence for the importance of NO in defining, in part, the hemocompatibility of biomaterials used in ECLS. However, even though the NORel polymer provides this preservation on platelets and maintain their ability to aggregate, this polymer has only a finite amount of NO that can be loaded and released over time during extracorporeal circulation (ECC). As presented here, the Cu^o-nanoparticle NO generating (NOGen) polymer plus a consistent supply of exogenous RSNOs (i.e., SNAP in this case), should provide a more continuous generation of NO at the blood/polymer interface. Indeed, via use of such a system, we have shown that platelet and monocyte counts are maintained not by

direct platelet P-selectin attenuation but possibly through a structural alteration of the plasma fibrinogen that prevents the functional aggregation of activated platelets. The only difference thought to exist between the Cu^o-nanoparticle NOGen polymer/SNAP system and the previously studied diazeniumdiolate-based NORel polymers is how NO is locally delivered to the blood and circulating platelets as well as monocytes flowing through the ECC. As previously reported, the degree of thrombosis and ECC-induced expression of platelet P-selectin and monocyte CD11b were attenuated with the NORel polymer [1] but, with the Cu^o-nanoparticle NOGen polymer/SNAP-configured system used in this work, the platelet P-selectin expression was not attenuated while the degree of ECC-induced thrombosis and monocyte CD11b expression were decreased similar to that observed with the NORel polymer systems. The underlying threshold level of locally-released NO from the Cu^o-nanoparticle NOGen polymers was concentration-dependent upon the wt.% of the Cu particle in the SP-60D-60 PU with a maximum NO released level of 12×10^{-10} mol cm^{-2} min^{-1} prior to and 10×10^{-10} mol cm^{-2} min^{-1}after 4 h of blood exposure achieved in the 10 wt.% Cu^o-nanoparticle polymer. Using this level of Cu^o-nanoparticle-containing polymer, our results further confirm our previous NORel data showing that this amount of NO flux nearly matches that seen with NORel, i.e., approx. 15×10^{-10} mol cm^{-2} min^{-1}. Interestingly, the lower concentrations of Cu^o-nanoparticles in the NOGen polymer (i.e., 1 and 5 wt.%) plus the SNAP infusion were not as effective in the *in vitro* NOA-measured NO release (5×10^{-10} and 8×10^{-10} mol cm^{-2} min^{-1}, respectively) or in the preservation of platelets as compared to the 10 wt.% Cu^o-nanoparticle NOGen polymer/SNAP effects. Although the *in vitro* NO generation level from the 10 wt.% Cu^o-nanoparticle NOGen polymer was similar to the level released by the previous NORel materials, there was a significant contrast in the *in vivo* levels of plasma fibrinogen and platelet function as measured by aggregometry and P-selectin upregulation. Interestingly, the *in vivo* combination of both the Cu catalyst in the ECC polymer and the added SNAP, was needed to maintain an environment of continuous NO release and the desired hemostatic effects. The level of plasma fibrinogen was reduced in all rabbit groups but the 10 wt.% Cu^o-nanoparticle polymer plus either the full or half-dose of SNAP and the 5 wt.% Cu polymer plus SNAP groups. The *in vitro* human fibrinogen immunoassay showed that fibrinogen adsorbed significantly to all the 1, 5 and 10 wt.% Cu^o-nanoparticle NOGen polymer surfaces and confirmed that the loss of rabbit plasma fibrinogen was more likely due to adsorption to the ECC surface in the non-Cu^o-nanoparticle/SNAP, 10 wt.% Cu^o-nanoparticle/saline or 1 wt.% Cu^o-nanoparticle/SNAP groups but not in the 5 and 10 wt.% Cu^o-nanoparticle ECC in the presence of the added SNAP. The increase in the *in vitro* fibrinogen adsorption is perhaps due to the roughness of the surface that develops with the Cu particles near the blood/polymer interface. However, the *in vivo* fibrinogen adsorption especially with the 10 wt.% Cu^o-nanoparticle ECC was in the presence of SNAP and the generated NO may prevent the fibrinogen from adsorbing in an as yet unclear mechanism (perhaps nitrosation of the protein). This issue warrants further investigation. In addition, in the 5 and 10 wt.% Cu^o-nanoparticle ECC plus the infused SNAP groups, platelet P-selectin upregulation was not attenuated as in the NORel polymer but remained unchanged from baseline, while the ability of the platelet to aggregate upon collagen stimulation was markedly reduced. This suggests that the added SNAP and high amount of Cu catalyst does not affect the platelet per se, but does influence an entity that is needed to promote platelet aggregation. The entity that may be affected by the Cu/SNAP combination could be the structure of plasma fibrinogen so that it is rendered unavailable for aggregating platelets.

Another aspect of the Cu catalyst/RSNO combination is the level of Cu(II) that leaches into the ECC blood due to copper particle corrosion and the excess RSNO, SNAP, that is infused intravenously. First, the corrosion rate for the 10 wt.% Cu^o-nanoparticle polymer in saline was found to be 11.4 + 4.1 μg/24 h. However, even after 7 d the rate was only 23.4 + 8.0 μg/7 d. To put this into perspective, the U.S. Institute of Medicine recommends the daily Cu

intake be 900 μg/day while the tolerable upper limit of intake to be 10,000 μg/day in adults [33]. Therefore, it is unlikely that in only 4 h of blood contact, even with a 10 wt.% copper particle-coated ECC circuit, that the level of Cu(II) leaching would reach anything close to toxic levels. The Cu(II) levels are actually less than 1% of the tolerated upper Cu intake level. Even though the Cu(II) levels are at well-tolerated levels, it is actually Cu(I) that is needed to generate NO from the RSNO. However, in cells and in blood, due to its highly reactive nature, Cu(I) is rapidly converted to Cu(II) via reaction with oxygen and other species. In addition, the vast majority of all copper ions within blood is complexed = to albumin and ceruloplasmin which carries 95% of the plasma copper ions and only 0.2 pM is in free Cu(II) or Cu(I) [34]. Any excess Cu(II) from the Cu ion leaching from the Cu^o-nanoparticle-containing ECC is ultimately taken up by ceruloplasmin or albumin but not before RSNO (SNAP) decomposition occurs within the hydrophilic PU coating. Secondly, the infused SNAP itself, which provides the ability of the Cu^o-containing ECC to release a continuous level of NO, may also have other biological effects. One of the prominent effects elicited by the systemic infusion of SNAP was marked hypotension. The co-administration of intravenous fluids counteracted the blood pressure fall but this could pose significant difficulties in a clinical situation. SNAP administration has been shown to cause hypotension [35], hyperglycemia [36] and decreased cell viability [37–39]. However, most of these adverse effects are ameliorated in the presence of endogenous thiols and superoxide dismutase. Future NOGen polymers should, therefore, reduce the need for systemic administration of RSNOs used in ECLS by co-incorporating a pool of RSNOs within the polymer coating, allowing the NO regeneration and nitrosation of reduced thiols to occur locally at the blood/polymer interface.

Not only does the aforementioned immobilized Cu particle-containing polymer and excess SNAP, generate NO, decrease thrombus formation, maintain platelet P-selectin expression upon collagen stimulation, and attenuate monocyte activation, but our results also show a marked influence on platelet aggregation and plasma fibrinogen Aαγ dimer assembly which all have a strong dependency on the level of Cu(II) and SNAP present. The generated NO from the Cu^o-nanoparticle ECC/SNAP combination appears to inhibit the functional ability of platelets to aggregate, but the platelets themselves still maintain the capacity to respond to prothrombotic agonists such as collagen as measured by the upregulation of P-selectin. As our previous work with the NORel polymer had shown, the P-selectin expression upon collagen stimulation is attenuated and followed the aggregometry response [1]. The question that arises is why is there a different response of the platelets for the NORel circuits and the currently studied Cu^o-nanoparticle NOGen ECC and added SNAP combination?. The important difference between the two NO producing ECC systems is the added SNAP. *S*-nitrosothiols, biologic molecules that serve an important role in the transport, storage and metabolism of NO, are sulfhydryl-containing plasma and cellular proteins that have reacted with and bound nitrosonium ions [40]. *S*-nitrosylation of cysteine residues within a broad functional spectrum of proteins constitute a large part of the ubiquitous influence of NO on physiological responses. The posttranslational modifications and functional regulation of both plasma and intracellular proteins is mediated through the *S*-nitrosylation mechanism [41]. Several proteins have been identified as *S*-nitrosylated proteins including soluble guanylate cyclase mediates production of intracellulear cyclic GMP (i.e., part of the NO-mediated cell signaling pathway) [42], platelet IIb/IIIa receptor binding to fibrinogen [43–45] and fibrinogen itself [25,46]. Geer et al. recently showed that glutathione and its derivatives including the nitrosated form, *S*-nitrosoglutathione, interact with several fibrinogen subunits especially the Aα subunit, alter its structure and inhibit fibrin polymerization upon activation [46]. Our results support their results by showing a reduction in the heterodimer Aαγ formation which is part of the early fibrin polymerization process. It is hypothesized that NO is transnitrosated from the infused SNAP to cysteines in the Aα and γ subunits of fibrinogen which explains our attenuated platelet aggregation but no effect on

the ability of the platelet to respond to collagen stimulation. Further studies are planned to verify this proposed mechanism.

5. Conclusions

This study has demonstrated that coating a solution of SP-60D-60 polyurethane containing copper (Cu) nanoparticles (25–50 nm) on PVC tubing can continuously generate and release NO for at least 4 h in a rabbit model of extracorporeal circulation. Significant amounts of NO generation appear to occur when an exogenous source of *S*-nitrosothiol is infused continuously (*S*-nitroso-*N*-acetylpenicillamine (SNAP)). The generation of NO, for example, from a10 wt.% Cu^{o}-nanoparticle doped polymer coating plus an exogenous infusion of the SNAP has been shown to preserve circulating platelets, both in count and function, as measured by P-selectin expression but not via aggregometry. The platelet count preservation appears to be promoted by direct effects on the structure of assembled plasma fibrinogen by the interaction of Cu(I) and SNAP to generate NO and not as much on the ability of platelets to be activated. These results indicate the potential of locally generating NO via the continuous interaction of Cu(I) ions with *S*-nitrosothiols to increase hemocompatibility of extracorporeal circuits and devices. In addition, this locally generated NO at the blood/polymer interface was found to be dependent upon the presence of both an exogenous source of RSNO and the copper catalyst, with dramatically less effect from including the RSNO source alone with the control coatings. Studies investigating improvements of the NOGen polymer in order to reduce the amount of exogenous RSNO administration systemically and Cu(II) leaching are planned for future studies. The NOGen polymer coatings described here have the potential to provide a and attractive approach in creating hemocompatible surfaces for a wide range of ECC-based therapies that cannot be fully addressed with direct NO releasing polymeric coatings (e.g., NORel).

Acknowledgments

The authors declare this work is supported by the National Institutes of Health, Grant #R01 HD 01534. M. E. Meyerhoff thanks the National Insitutes of Health, Grant EB-004527, for supporting fundamental chemistry studies on the preparation and characterization of NO generating polymeric coatings. The authors except Dr. Robert Bartlett confirm that there are no known conflicts of interest associated with this publication and there has been no significant financial support for this work that could have influenced its outcome. Dr. Robert Bartlett has an equity interest in Accord Biomaterials, Inc. but no financial support from this company was utilized in any of this paper's work.

References

[1]. Major TC, Brant DO, Reynolds MM, Bartlett RH, Meyerhoff ME, Handa H, et al. The attenuation of platelet and monocyte activation in a rabbit model of extracorporeal circulation by a nitric oxide releasing polymer. Biomaterials. 2010; 31:2736–45. [PubMed: 20042236]

[2]. Frost MC, Reynolds MM, Meyerhoff ME. Polymers incorporating nitric oxide releasing/generating substances for improved biocompatibility of blood-contacting medical devices. Biomaterials. 2005; 26:1685–93. [PubMed: 15576142]

[3]. Reynolds MM, Frost MC, Meyerhoff ME. Nitric oxide-releasing hydrophobic polymers: preparation, characterization, and potential biomedical applications. Free Radic Biol Med. 2004; 37:926–36. [PubMed: 15336308]

[4]. Batchelor MM, Reoma SL, Fleser PS, Nuthakki VK, Callahan RE, Shanley CJ, et al. More lipophilic dialkyldiamine-based diazeniumdiolates: synthesis, characterization, and application in preparing thromboresistant nitric oxide release polymeric coatings. J Med Chem. 2003; 46:5153–61. [PubMed: 14613318]

[5]. Annich GM, Meinhardt JP, Mowery KA, Ashton BA, Merz SI, Hirschl RB, et al. Reduced platelet activation and thrombosis in extracorporeal circuits coated with nitric oxide release polymers. Crit Care Med. 2000; 28:915–20. [PubMed: 10809259]

[6]. Hwang S, Meyerhoff ME. Polyurethane with tethered copper(II)-cyclen complex: preparation, characterization and catalytic generation of nitric oxide from S-nitrosothiols. Biomaterials. 2008; 29:2443–52. [PubMed: 18314189]

[7]. Wu Y, Rojas AP, Griffith GW, Skrzypchak AM, Lafayette N, Bartlett RH, et al. Improving blood compatibility of intravascular oxygen Sensors via catalytic decomposition of *S*-Nitrosothiols to generate nitric oxide in. Situ. Sens Actuators B Chem. 2007; 121:36–46. [PubMed: 17330157]

[8]. Frost MC, Meyerhoff ME. Synthesis, characterization, and controlled nitric oxide release from *S*-nitrosothiol-derivatized fumed silica polymer filler particles. J Biomed Mater Res A. 2005; 72:409–19. [PubMed: 15682428]

[9]. Oh BK, Meyerhoff ME. Spontaneous catalytic generation of nitric oxide from *S*-nitrosothiols at the surface of polymer films doped with lipophilic copperII complex. J Am Chem Soc. 2003; 125:9552–3. [PubMed: 12903997]

[10]. Scharfstein JS, Keaney JF Jr, Slivka A, Welch GN, Vita JA, Stamler JS, et al. In vivo transfer of nitric oxide between a plasma protein-bound reservoir and low molecular weight thiols. J Clin Invest. 1994; 94:1432–9. [PubMed: 7929818]

[11]. Burg A, Cohen H, Meyerstein D. The reaction mechanism of nitrosothiols with copper(I). J Biol Inorg Chem. 2000; 5:213–7. [PubMed: 10819466]

[12]. Hogg N. Biological chemistry and clinical potential of *S*-nitrosothiols. Free Radic Biol Med. 2000; 28:1478–86. [PubMed: 10927172]

[13]. Tsikas D, Sandmann J, Rossa S, Gutzki FM, Frolich JC. Investigations of *S*-transnitrosylation reactions between low- and high-molecular-weight *S*-nitroso compounds and their thiols by high-performance liquid chromatography and gas chromatography-mass spectrometry. Anal Biochem. 1999; 270:231–41. [PubMed: 10334840]

[14]. Stubauer G, Giuffre A, Sarti P. Mechanism of *S*-nitrosothiol formation and degradation mediated by copper ions. J Biol Chem. 1999; 274:28128–33. [PubMed: 10497164]

[15]. Dicks AP, Williams DL. Generation of nitric oxide from *S*-nitrosothiols using protein-bound Cu2+ sources. Chem Biol. 1996; 3:655–9. [PubMed: 8807899]

[16]. Massaguer A, Engel P, Perez-del-Pulgar S, Bosch J, Pizcueta P. Production and characterization of monoclonal antibodies against conserved epitopes of P-selectin (CD62P). Tissue Antigens. 2000; 56:117–28. [PubMed: 11019911]

[17]. Welt FG, Edelman ER, Simon DI, Rogers C. Neutrophil, not macrophage, infiltration precedes neointimal thickening in balloon-injured arteries. Arterioscler Thromb Vasc Biol. 2000; 20:2553–8. [PubMed: 11116052]

[18]. Brodersen R, Bijlsma F, Gori K, Jensen KT, Chen W, Dominguez J, et al. Analysis of the immunological cross reactivities of 213 well characterized monoclonal antibodies with specificities against various leucocyte surface antigens of human and 11 animal species. Vet Immunol Immunopathol. 1998; 64:1–13. [PubMed: 9656427]

[19]. Jacobsen CN, Aasted B, Broe MK, Petersen JL. Reactivities of 20 anti-human monoclonal antibodies with leucocytes from ten different animal species. Vet Immunol Immunopathol. 1993; 39:461–6. [PubMed: 8116221]

[20]. Grunkemeier JM, Tsai WB, McFarland CD, Horbett TA. The effect of adsorbed fibrinogen, fibronectin, von Willebrand factor and vitronectin on the procoagulant state of adherent platelets. Biomaterials. 2000; 21:2243–52. [PubMed: 11026630]

[21]. Vaughn MW, Kuo L, Liao JC. Estimation of nitric oxide production and reaction rates in tissue by use of a mathematical model. Am J Phys. 1998; 274:H2163–76.

[22]. Andrews RK, Berndt MC. Platelet physiology and thrombosis. Thromb Res. 2004; 114:447–53. [PubMed: 15507277]

[23]. Ilmakunnas M, Pesonen EJ, Ahonen J, Ramo J, Siitonen S, Repo H. Activation of neutrophils and monocytes by a leukocyte-depleting filter used throughout cardiopulmonary bypass. J Thorac Cardiovasc Surg. 2005; 129:851–9. [PubMed: 15821654]

[24]. Huang S, Mulvihill ER, Farrell DH, Chung DW, Davie EW. Biosynthesis of human fibrinogen. Subunit interactions and potential intermediates in the assembly. J Biol Chem. 1993; 268:8919–26. [PubMed: 8473334]

[25]. Akhter S, Vignini A, Wen Z, English A, Wang PG, Mutus B. Evidence for *S*-nitrosothiol-dependent changes in fibrinogen that do not involve transnitrosation or thiolation. Proc Natl Acad Sci U S A. 2002; 99:9172–7. [PubMed: 12089331]

[26]. Bor-Kucukatay M, Keskin A, Akdam H, Kabukcu-hacioglu S, Erken G, Atsak P, et al. Effect of thrombocytapheresis on blood rheology in healthy donors: role of nitric oxide. Transfus Apher Sci. 2008; 39:101–8. [PubMed: 18707921]

[27]. Skrzypchak AM, Lafayette NG, Bartlett RH, Zhou Z, Frost MC, Meyerhoff ME, et al. Effect of varying nitric oxide release to prevent platelet consumption and preserve platelet function in an in vivo model of extracorporeal circulation. Perfusion. 2007; 22:193–200. [PubMed: 18018399]

[28]. Adrian K, Skogby M, Friberg LG, Mellgren K. The effect of s-nitroso-glutathione on platelet and leukocyte function during experimental extracorporeal circulation. Artif Organs. 2003; 27:570–5. [PubMed: 12780512]

[29]. Skogby M, Friberg LG, Adrian K, Mellgren K. Pharmacological inhibition of plasma coagulation and platelet activation during experimental long-term perfusion. Scand Cardiovasc J. 2003; 37:222–8. [PubMed: 12944211]

[30]. Zhang H, Annich GM, Miskulin J, Osterholzer K, Merz SI, Bartlett RH, et al. Nitric oxide releasing silicone rubbers with improved blood compatibility: preparation, characterization, and in vivo evaluation. Biomaterials. 2002; 23:1485–94. [PubMed: 11829445]

[31]. Mellgren K, Friberg LG, Mellgren G, Hedner T, Wennmalm A, Wadenvik H. Nitric oxide in the oxygenator sweep gas reduces platelet activation during experimental perfusion. Ann Thorac Surg. 1996; 61:1194–8. [PubMed: 8607682]

[32]. Mellgren K, Friberg LG, Hedner T, Mellgren G, Wadenvik H. Blood platelet activation and membrane glycoprotein changes during extracorporeal life support (ECLS). In vitro studies. Int J Artif Organs. 1995; 18:315–21. [PubMed: 8593966]

[33]. Stern BR. Essentiality and toxicity in copper health risk assessment: overview, update and regulatory considerations. J Toxicol Environ Health A. 2010; 73:114–27. [PubMed: 20077283]

[34]. Tapiero H, Townsend DM, Tew KD. Trace elements in human physiology and pathology. Copper Biomed Pharmacother. 2003; 57:386–98.

[35]. Rassaf T, Kleinbongard P, Preik M, Dejam A, Gharini P, Lauer T, et al. Plasma nitrosothiols contribute to the systemic vasodilator effects of intravenously applied NO: experimental and clinical Study on the fate of NO in human blood. Circ Res. 2002; 91:470–7. [PubMed: 12242264]

[36]. McGrowder D, Ragoobirsingh D, Dasgupta T. Effects of *S*-nitroso-N-acetylpenicillamine administration on glucose tolerance and plasma levels of insulin and glucagon in the dog. Nitric Oxide. 2001; 5:402–12. [PubMed: 11485378]

[37]. Fatokun AA, Stone TW, Smith RA. Prolonged exposures of cerebellar granule neurons to *S*-nitroso-N-acetylpenicillamine (SNAP) induce neuronal damage independently of peroxynitrite. Brain Res. 2008; 1230:265–72. [PubMed: 18644353]

[38]. Khalil-Manesh F, Price RG. Effect of D-penicillamine on glomerular basement membrane, urinary N-acetyl-beta-D-glucosaminidase and protein excretion in rats. Toxicology. 1983; 26:325–34. [PubMed: 6857704]

[39]. Zamora R, Matthys KE, Herman AG. The protective role of thiols against nitric oxide-mediated cytotoxicity in murine macrophage J774 cells. Eur J Pharmacol. 1997; 321:87–96. [PubMed: 9083790]

[40]. Stamler JS, Simon DI, Osborne JA, Mullins ME, Jaraki O, Michel T, et al. *S*-nitrosylation of proteins with nitric oxide: synthesis and characterization of biologically active compounds. Proc Natl Acad Sci U S A. 1992; 89:444–8. [PubMed: 1346070]

[41]. Foster MW, Hess DT, Stamler JS. Protein *S*-nitrosylation in health and disease: a current perspective. Trends Mol Med. 2009; 15:391–404. [PubMed: 19726230]

[42]. Sayed N, Kim DD, Fioramonti X, Iwahashi T, Duran WN, Beuve A. Nitroglycerin-induced *S*-nitrosylation and desensitization of soluble guanylyl cyclase contribute to nitrate tolerance. Circ Res. 2008; 103:606–14. [PubMed: 18669924]

[43]. Federico A, Filippelli A, Falciani M, Tuccillo C, Tiso A, Floreani A, et al. Platelet aggregation is affected by nitrosothiols in patients with chronic hepatitis: in vivo and in vitro studies. World J Gastroenterol. 2007; 13:3677–83. [PubMed: 17659726]

[44]. Walsh GM, Leane D, Moran N, Keyes TE, Forster RJ, Kenny D, et al. *S*-Nitrosylation of platelet alphaIIbbeta3 as revealed by Raman spectroscopy. Biochemistry. 2007; 46:6429–36. [PubMed: 17474714]

[45]. Oberprieler NG, Roberts W, Riba R, Graham AM, Homer-Vanniasinkam S, Naseem KM. cGMP-independent inhibition of integrin alphaIIbbeta3-mediated platelet adhesion and outside-in signalling by nitric oxide. FEBS Lett. 2007; 581:1529–34. [PubMed: 17376438]

[46]. Geer CB, Stasko NA, Rus IA, Lord ST, Schoenfisch MH. Influence of glutathione and its derivatives on fibrin polymerization. Biomacromolecules. 2008; 9:1876–82. [PubMed: 18570468]

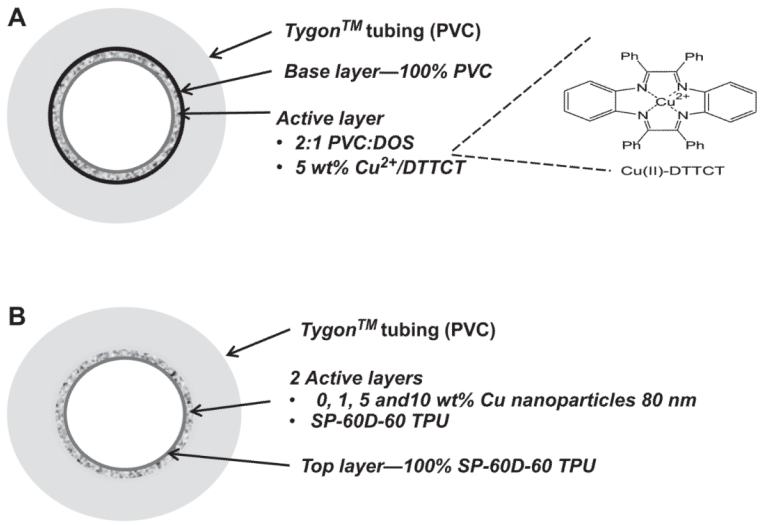

Fig. 1.

NO generating (NOGen) fabrication. (A) Schematic of polymer containing a lipophilic Cu(II) complex (analogue to cyclen) (Cu(II)-dibenzo[e,k]-2,3,8,9-tetraphenyl-1,4,7,10-tetraaza-cyclododeca-1,3,7,9-tetraene (Cu(II)-DTTCT)) and incorporated at 5 wt.% into plasticized PVC. This was coated as 1 active layer on PVC tubing. (B) Schematic of SP-60D-60 polyurethane containing 25–50 nm copper nanoparticles that is layered as 2 active coats on PVC tubing.

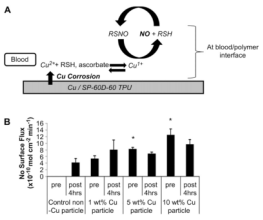

Fig. 2.

(A) A working hypothesis of the NO release from circulating RSNO which is catalyzed by Cu(I) ions that are reduced from Cu(II) ions released through corrosion of the copper particle in polymer. (B) NO releasing characteristics as measured by NOA chemiluminescence. NO surface flux prior to and after 4 h of blood exposure. The data are means ± SEM. Significance was determined at a $p < 0.05$.

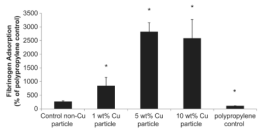

Fig. 3.

In vitro fibrinogen adsorption assay on 1, 5 and 10 wt.% Cu^{o}-nanoparticle-based NOGen and control polymers. Fluorescence assay in a 96-well format that used a goat anti-human fibrinogen-FITC conjugated antibody to measure the level of adsorbed human fibrinogen (3 μg/ml) to plated NOGen and control polymers. The data are means ± SEM. * = $p < 0.05$, control vs NOGens.

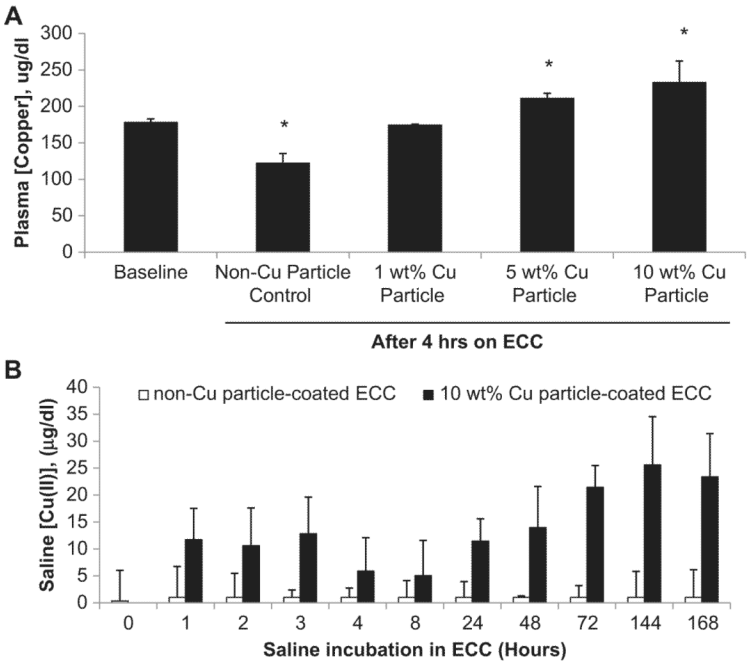

Fig. 4.

Plasma copper concentration assay. (A) Quantitation of the total copper concentration in plasma of the various wt.% Cu^0-nanoparticle-containing NOGen and control polymers prior to and 4 h after ECC blood exposure. (B) *In vitro* time course of copper ion leaching from 10 wt.% NOGen and control polymers after 7 d in saline. The data are means ± SEM. * = $p < 0.05$, control vs NOGens.

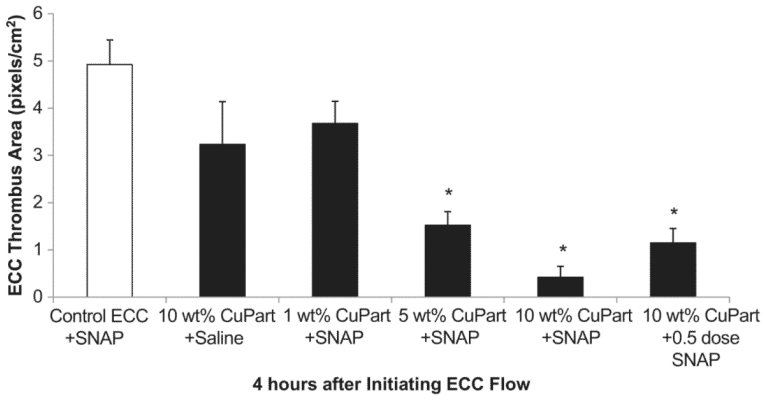

Fig. 5.

Thrombus formation of 1, 5 and 10 wt.% Cu^0-nanoparticle doped NOGen and control polymer ECCs with and without SNAP infusion after 4 h blood exposure in the rabbit thrombogenicity model. Quantitation of the thrombus area as calculated using Image J software from NIH. The data are means ± SEM. * = $p < 0.05$, control ECC plus SNAP vs NOGen ECCs after 4 h.

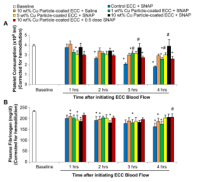

Fig. 6.

Time-dependent effects of NOGen polymer ECC on rabbit platelet count (i.e., consumption) (A) and plasma fibrinogen levels (B) after 4 h of blood exposure in rabbit thrombogenicity model. Data is the mean ± SEM. * = $p < 0.05$, baseline vs control + SNAP and NOGen ECCs. # = $p < 0.05$, control ECC + SNAP vs NOGen ECCs.

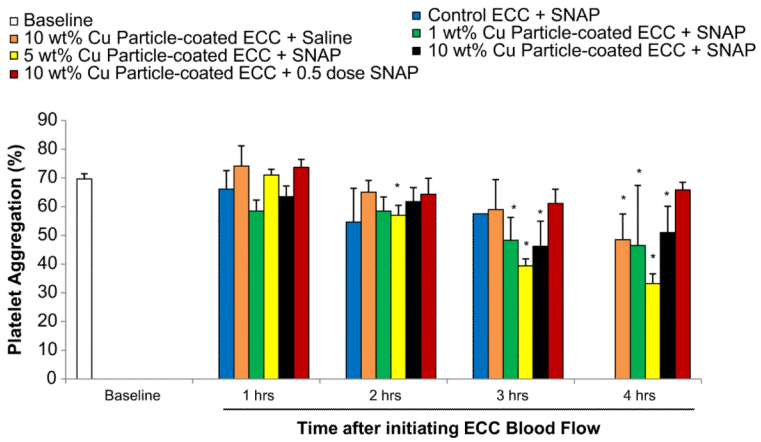

Fig. 7.

Time course of platelet aggregometry as measured by optical turbidity. Platelet-rich plasma was prepared and the aggregation initiated by 10 μg/ml collagen. The data are means ± SEM. * = $p < 0.05$, baseline vs control and NOGen ECCs.

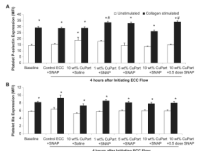

Fig. 8.

Fluorescent-activated cell sorting (FACS) analysis for circulating platelet P-selectin (CD62P) after 4 h blood exposure with NOGen or control polymer-coated ECCs ± exogenous SNAP. (A) Platelet P-selectin mean fluorescence intensity (MFI) after 4 h on ECC with or without 40 μg/ml collagen stimulation in NOGen and control polymers. (B) Platelet IIIa (CD61), subunit of the platelet fibrinogen receptor, mean fluorescence intensity (MFI) after 4 h on ECC with or without 40 μg/ml collagen stimulation in NOGen and control polymers. The data are means ± SEM. * = $p < 0.05$, unstimulated vs collagen-stimulated for baseline, control ECC and NOGen ECCs. # = $p < 0.05$, collagen-stimulated for baseline vs collagen-stimulated for control ECC and collagen-stimulated for NOGen ECCs. The specific MFI data is after the isotype control value was subtracted from each P-selectin MFI value. All FACS analyses used the gated FSC/SSC plot for platelets and 100 μl of diluted whole rabbit blood (1:100) was used for each determination.

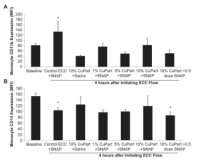

Fig. 9.

Fluorescent-activated cell sorting (FACS) analysis for circulating monocytes after 4 h blood exposure with NOGen or control polymer-coated ECCs with or without exogenous SNAP infusion. (A), Monocyte CD11b mean fluorescence intensity (MFI) after 4 h on ECC in NOGen and control polymers. (B) Monocyte CD14 (monocyte specific marker) mean fluorescence intensity (MFI) after 4 h on ECC in NOGen and control polymers. The data are means ± SEM. * = $p < 0.05$, baseline vs control ECC or NOGen ECCs. The specific MFI data is after the isotype control value was subtracted from each CD11b or CD14 MFI value. All FACS analyses used the gated FSC/SSC plot for monocytes and 100 μl of whole rabbit blood was used for each determination.

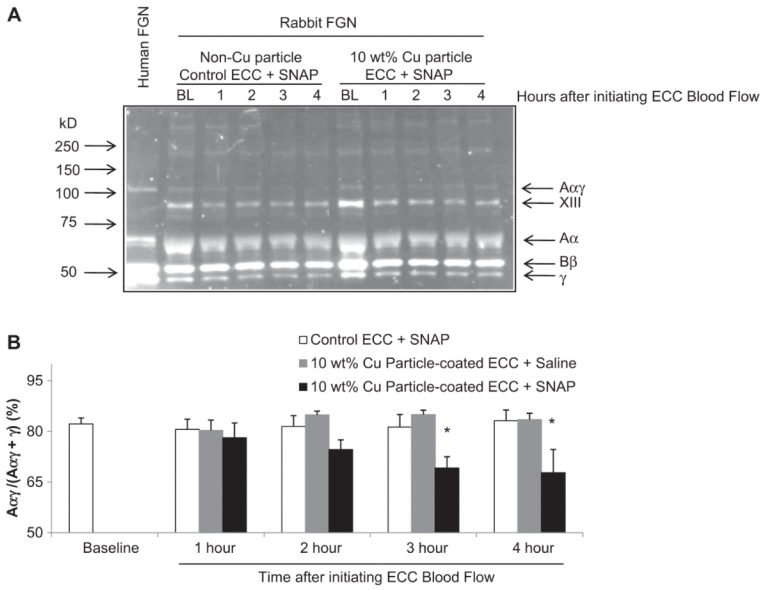

Fig. 10.

Western immunoblot analysis of rabbit plasma fibrinogen after 4 h blood exposure with 10 wt.% Cu^{o}-nanoparticle NOGen ± exogenous SNAP or control polymer-coated ECCs plus exogenous SNAP. (A), Representative immunoblot. Aliquots (0.2 μl) of reduced plasma samples after 4 h on ECCs in NOGen or control polymers were separated on 7.5% polyacrylamide gels, protein transferred to poly(vinyl-difluoride) (PVDF) membranes and then immunostained with FITC conjugated goat anti-human fibrinogen antibody. Human plasma fibrinogen was used to confirmed cross-reactivity of the anti-human antibody to rabbit plasma fibrinogen. FGN = fibrinogen. Molecular weight markers are shown on left with positions of the relevant fibrinogen chains and factor XIII indicated on the right. (B) Western blot of plasma samples in (A), after 4 h on ECC in NOGen and control polymers, were quantified by densitometry using Quanity One imaging software (Bio-Rad Hercules, CA). The specific Aαγ dimer formation was calculated as the ratio (density) of the Aαγ dimer band over the sum of dimers plus monomers. The data are means ± SEM. * = $p <$ 0.05, baseline vs control ECC/SNAP or 10 wt.% Cu particle NOGen ECCs/± SNAP.

Table 1

Effects of 10 wt.% NO generating polymer (NOGen) plus exogenous SNAP infusion on hemodynamic parameters in the rabbit model of extracorporeal circuits (ECC).

Treatment	Parameter	Baseline[a]	Time on ECC (hours)			
			1	2	3	4
Control polymer ECC + SNAP infusion	MAP	76 ± 2 (32)	36 ± 1 (7)*	68 ± 19 (7)	69 ± 13 (7)	84 ± 10 (7)
	HR	208 ± 7 (32)	209 ± 7 (7)	213 ± 13 (7)	231 ± 6 (7)	242 ± 4 (7)*
	ECC BF	94 ± 3 (32)	74 ± 11 (7)	134 ± 20 (7)*	145 ± 13 (7)*	185 ± 9 (6)*
	ACT	169 ± 4 (32)	156 ± 4 (7)	186 ± 10 (7)	210 ± 9 (7)*	220 ± 12 (7)*
	WBC count	3504 ± 115 (32)	3195 ± 425 (7)	2844 ± 268 (7)	2672 ± 384 (7)	2515 ± 347 (7)
10 wt.% NOGen polymer ECC + SNAP infusion	MAP	76 ± 2 (32)	34 ± 2 (6)*	46 ± 6 (6)*	76 ± 11 (6)	97 ± 10 (6)*
	HR	208 ± 7 (32)	209 ± 4 (6)	201 ± 8 (6)	222 ± 18 (6)	223 ± 16 (6)
	ECC BF	94 ± 3 (32)	75 ± 7 (6)	105 ± 15 (6)	145 ± 19 (6)*	174 ± 21 (6)*
	ACT	169 ± 4 (32)	162 ± 6 (6)	183 ± 11 (6)	202 ± 16 (6)*	208 ± 22 (6)*
	WBC count	3504 ± 115 (32)	3216 ± 348 (6)	4044 ± 895 (6)	3423 ± 693 (6)	3722 ± 910 (6)

Values are means ± SEM. () = *n* size.

* $p < 0.05$ vs baseline; ANOVA with Student's *t* multirange test.

[a] Values are prior to ECC placement. MAP = mean arterial pressure (mmHg), HR = heart rate (beats/min), BF = blood flow (ml/min), ACT = activated clotting time (sec), WBC = white blood cells.